Effects of Bortezomib on Human Neuroblastoma Cells *In Vitro* and in a Metastatic Xenograft Model

URSULA VALENTINER, CHRISTINA HAANE, NINA NEHMANN and UDO SCHUMACHER

Institute for Anatomy II: Experimental Morphology, University Hospital Hamburg-Eppendorf, Hamburg, Germany

Abstract. *Background: Inhibition of the proteasome-ubiquitin pathway has shown to exert growth inhibitory effects on several human carcinoma cell lines. In this study, the influence of bortezomib on human neuroblastoma cells was investigated. Materials and Methods: Cell proliferation of seven human neuroblastoma cell lines under bortezomib treatment was assessed by a colorimetric XTT-based assay. Subsequently, the influence of bortezomib on SK-N-SH neuroblastoma cell growth was examined in a spontaneous metastatic SCID mouse model. Results: In vitro, bortezomib inhibited proliferation of all cell lines in a dose-dependent manner. In the xenograft model, bortezomib treatment did not have an effect on the tumour weight, but induced apoptosis and reduced mitosis and angiogenesis, as well as the formation of pulmonary metastases. Conclusion: Bortezomib has anticancer effects on neuroblastoma cells in vitro and in a metastatic xenograft model. These findings provide a basis for further investigations of bortezomib in the treatment of metastasising neuroblastoma.*

Neuroblastoma arises from embryonic neural crest cells, which can occur anywhere along the strands of the sympathetic nervous system. It is the most common extracranial solid tumour in childhood (1). Although spontaneous regression can occur in children less than one year old, 70% of patients over the age of one year present with high-risk and difficult-to-treat neuroblastoma at diagnosis, characterized by the presence of distant metastases and in some cases by amplification of the *N-myc* oncogene. Despite the use of multimodality therapeutic protocols for high-risk neuroblastoma patients, long-term survival of

Correspondence to: Dr. Ursula Valentiner, Institute for Anatomy II: Experimental Morphology, University Hospital Hamburg-Eppendorf, Martinistr. 52, D-20246 Hamburg, Germany. Tel: +49 40 741053587, Fax: +49 40 741055427, e-mail: valentin@uke.uni-hamburg.de

Key Words: neuroblastoma, proteasome inhibitor, bortezomib, metastases, xenograft model.

children with stage 4 neuroblastoma still remains less than 40% (1-4). Thus, the search for new agents with therapeutic potential in high-risk neuroblastoma is of considerable clinical interest. Human tumour cell xenograft models using immunodeficient mice have provided an *in vivo* model system for the study of new therapeutic agents in cancer research. Previous experiments with human breast and colon cancer and melanoma have shown that the transplantation of cancer cells into SCID mice presents a model system of particular clinical relevance (5-8).

One attractive target for the development of novel anticancer therapies is proteasome inhibition. The ubiquitin-proteasome pathway controls the intracellular protein turnover and is involved in apoptosis, transcription, cell adhesion, angiogenesis, antigen presentation and cell cycle (9). Tumour cells seem to be more sensitive to these effects of proteasome inhibition than are normal cells and undergo apoptosis under the influence of proteasome inhibitors such as bortezomib (10). Bortezomib, the first proteasome inhibitor to reach clinical practice, is a water soluble dipeptide that binds to the proteasome with very high affinity and dissociates slowly, imparting stable but reversible proteasome inhibition (11). Bortezomib has shown *in vitro* and *in vivo* activity against a variety of malignancies, including myeloma, mantle cell lymphoma, non-small cell lung carcinoma, and ovarian, pancreatic, prostate and head and neck cancer (12-21).

Recent studies have already shown that bortezomib is an inhibitor of neuroblastoma cell proliferation (22-24). However, the influence on the metastatic potential of neuroblastoma cells has not been investigated so far. In this study, the effect of the proteasome inhibitor bortezomib on seven well-established human neuroblastoma cell lines *in vitro* and in a spontaneous metastatic neuroblastoma xenograft model has been examined.

Materials and Methods

Cell lines. Seven human neuroblastoma cell lines, namely Kelly, LS, SH-SY5Y, SK-N-SH, IMR-32, LAN-1 and LAN-5 were used. Kelly, LAN-1, LAN-5, SK-N-SH and IMR-32 were obtained from Prof. Dr. Rudolf Erttmann (Department of Pediatric Oncology,

University Hospital Hamburg-Eppendorf, Germany); LS and SH-SY5Y from Prof. Dr. Reinhard Hildebrandt (Abteilung Zelluläre Chemie, Medizinsche Hochschule Hannover, Germany). Cells were cultured *in vitro* under standard cell culture conditions (37°C, 100% relative humidity, 5% CO_2) in RPMI medium (Gibco/Life Technologies, Paisley, Scotland) supplemented with 10% heat-inactivated fetal bovine serum (FBS, Gibco), 2 mM L-glutamine (Gibco), 100 U/ml penicillin and 100 μg/ml streptomycin (Gibco). Before reaching confluency, cells were routinely harvested for passaging using 0.05% trypsin-0.02% EDTA (Gibco).

Bortezomib (Velcade®). Bortezomib (Velcade®) was purchased through the hospital pharmacy from Janssen-Cilag (Neuss, Germany). Bortezomib was dissolved in phosphate buffered saline (PBS) and a stock solution of 1 mg/ml was produced and stored at –20°C until use.

Cell proliferation assay. Cell proliferation was quantified using the colorimetric XTT-based assay kit (Boehringer Mannheim, Mannheim, Germany). Cells were detached with trypsin, washed and transferred into 96-well microtitre plates (Greiner, Frickenhausen, Germany) at a density of $15×10^4$ cells/ml (Kelly and LAN-1), $7×10^4$ cells/ml (LS), $20×10^4$ cells/ml (LAN-5), $42×10^4$ cells/ml (SH-SY5Y), $6×10^4$ cells/ml (SK-N-SH) and $70×10^4$ cells/ml (IMR-32). All cells were incubated for 24 h before administration of bortezomib diluted in PBS. The final test concentrations were 0.0002, 0.002, 0.02, 0.2, 2 and 20 μg/ml bortezomib. Each concentration was fivefold tested and at least four independent experiments were carried out. The control cells received RPMI with 0.1 M PBS instead of bortezomib. Cells were incubated for 48 h and then 50 μl XTT solution were added for 6 h (IMR-32, Kelly, LAN-1, LAN-5, LS, SK-N-SH) or 24 h (SH-SY5Y) at 37°C. Absorbance was measured at 490 nm in a Dynatech MR 3.13 Microelisa Reader (Dynex Technologies, Ashford, UK).

The effect of bortezomib on the cell proliferation of the seven cell lines was studied as a dose–response experiment. Absorbance of untreated controls corresponded to 100% survival, absorbance of treated cells was taken as percentage of viable cells relative to the control. The effect of bortezomib on cell proliferation was presented for each concentration as the mean±SEM determined of at least four independent experiments.

Cell migration. To investigate the activity of SK-N-SH cell motility under treatment with bortezomib, a modified scratch wound assay was used. SK-N-SH cells were grown to confluence in multiwell dishes (Nunc, Roskilde, Denmark) with culture inserts (Ibidi, Martinsried, Germany) leaving a definite cell-free gap of approximately 400 μm. The cells were washed with PBS before their incubation in culture medium in the absence (control) or presence of bortezomib (5 and 10 ng/ml). The colonization of the cell-free gap was analysed and photographed 0, 8, 20 and 28 h after cell treatment with a Zeiss Axiovert 200 cell culture microscope (Zeiss, Oberkochen, Germany). The migration rate was calculated digitally by quantification of the cell-free area at the different time points using the AxioVision program (Zeiss). The experiments were performed in duplicate and repeated three times.

In vivo therapeutic study. For the therapeutic studies, 15-week-old male and female SCID mice, weighing on average 25 g (SEM±0.5

g) at the beginning of the experiments, were used. They were housed in filter top cages, provided with sterile water and food *ad libitum* and treated according to institutional care protocols. The animal testing was approved by the local animal experiment approval committee (Behörde für Soziales, Familie, Gesundheit, Verbraucherschutz; Amt für Gesundheit und Verbraucherschutz, Hamburg, Germany) and assigned the project No. 64/05.

All manipulations were carried out aseptically inside a laminar flow hood. For injection, SK-N-SH neuroblastoma cells were harvested by trypsination and viable cells ($5×10^6$) were suspended in 1 ml cell culture medium. An aliquot of 200 μl of this suspension was injected subcutaneously between the scapulae of each SCID mouse. The mice were divided into two groups of 20 mice, respectively. Mice of the control group received 200 μl saline and mice of the treated group 1 mg/kg bortezomib in 200 μl saline. Treatment *via* injections into the tail vein began three days after cell inoculation and continued twice a week for a total of 28 days. General physical status of the animals was regularly recorded; no signs of impairment of the animals caused by the medical treatment were noted. Thirty one days after cell inoculation mice were terminally anesthetized with intraperitoneal injections of 0.1 ml/10 g body weight Rompun/Ketanest (0.8 ml Rompun 2% (Bayer, Leverkusen, Germany), 1.2 ml Ketamin Gräub (100 mg/ml (Albrecht, Aulendorf, Germany) in 8 ml 0.9% NaCl)) and blood samples were taken from the retroorbital venous plexus, transferred in EDTA micro tubes (Sarstedt, Nümbrecht, Germany) and stored at 4°C until use for DNA extraction. Finally the mice were killed by cervical dislocation and the primary tumours were removed, weighed and fixed in 10% PFA in PBS. The lungs were dissected out *en bloc* and fixed in 10% PFA in PBS for investigation of the presence of pulmonary metastases.

Histology. Fixed primary tumours were processed to paraffin wax and 5 μm sections were stained with hematoxylin-eosin (HE). The slides were investigated for the percentage of necrotic areas, apoptotic cells (cell shrinkage and condensed nuclei) and mitotic cells (mitotic figures with condensed chromosomes). Apoptotic cells were determined as described by Kerr *et al*. (25), who have set the most exact method to analyse apoptotic rates in comparison with other methodological approaches (26). For the quantitative assessment of apoptosis and mitosis, 100 cells were examined in 15 different microscopic fields (magnification ×400) in one representative slide of each tumour (27). Mitotic, apoptotic and normal cells were counted and the percentage of apoptotic and mitotic cells was recorded. The dimension of necrotic areas in the primary tumours was evaluated according to the morphological criteria described by Kerr *et al*. (25) and measured digitally using the AxioVision program (Zeiss).

The lungs were cut into about 1 mm-thick slices, which were spread randomly over a glass slide and were embedded in 4% agar (Agar Noble; Difco Laboratories, Detroit, MI, USA). The solidified agar blocks were subsequently processed for routine wax histology and serially sectioned. The number of pulmonary metastases was determined as previously described by Jojovic and Schumacher (28). Briefly, every tenth section was retained and ten sections from the middle of the block were stained with hematoxylin-eosin. All metastases found in one section were counted (magnification ×100) and the mean value of the ten sections (mean value10) was calculated. This mean value10 minus 20% was multiplied by the total number of serial sections in order to achieve an estimated value for the total number of lung metastases (28).

Table I. *Bortezomib concentration that caused 50% inhibition of cell proliferation (IC_{50} values) in seven human neuroblastoma cell lines.*

Cell line	SH-SY5Y	SK-N-SH	IMR-32	LAN-5	LAN-1	LS	Kelly
IC_{50} ng/ml (95% CI)	1.2 (0.9-1.6)	5.5 (4.3-7.0)	5.9 (4.5-7.7)	7.3 (6.0-8.9)	8.2 (6.6-10.2)	6.4 (5.1-8.2)	6.2 (4.7-8.0)

95% CI=95% Confidence interval.

CD31 immunohistochemistry. For antigen retrieval, sections of the primary tumours were dewaxed and treated with proteinase K (0.5 mg/ml, Merck, Darmstadt, Germany) for 15 min at 37˚C. Non-specific binding was blocked by 10% normal rabbit serum (Dako) followed by incubation overnight at 4˚C with the monoclonal anti-mouse CD31 antibody (Biermann, Hiddenhausen, Germany) diluted 1:25 in Dako diluent. Subsequently, slides were incubated with biotinylated rabbit anti-rat antibody for 30 min at room temperature. This was followed by incubation with an avidin-alkaline phospatase complex (Vectastain, ABC kit; Vector Laboratories, Burlingame, USA). Enzyme reactivity of the alkaline phosphate complex was visualized using Naphtol-AS-biphosphate as a substrate and hexatozised New Fuchsin was used for simultaneous coupling. Slides were rinsed in tap water, covered with Crystal Mount and Clarion (Biomeda, Foster City, California, USA) and were examined under a Zeiss Axioplan photomicroscope.

Tumour microvessel densitiy (MVD) in vital tumour tissue was calculated as a mean of CD31-positive vessel counts in three fields of view determined in two representative tumour sections, respectively. Each field of view corresponded to an area of 0.625 mm × 0.625 mm.

Negative controls were treated the same way, omitting the incubation step with the primary antibody, and showed no immuno-reactivity.

Real-time PCR. In order to detect human tumour cells in the bloodstream, quantification of human tumour cell DNA *via* Alu-sequences was carried out (29). In brief, real-time polymerase chain reaction (PCR) and melting curve analyses were performed in glass capillaries with the LightCycler® 2.0 System. For the real-time PCR the LightCycler Fast Start DNA MasterPLUS SYBRGreen I Kit (Roche Diagnostics GmbH, Mannheim, Germany) was used. Two μl DNA of a whole blood cell extract obtained by QIAmp DNA Blood Mini Kit (Qiagen) was used as a template for the PCR reaction and incubated in a total reaction volume of 10 μl, containing 1 x SYBR Green I Master mix including Taq DNA polymerase, Taq PCR buffer, a dNTP mixture and 1 mmol/l $MgCl_2$, 10 pmol specific Alu primers. Forward Alu primer (TGG CTC ACG CCT GTA ATC CCA) and reverse Alu primer (GCC ACT ACG CCC GGC TAA TTT) were synthesized by MWG-BIOTECH AG (Ebersberg, Germany). The PCR conditions were initially 10 min 95˚C, followed by 50 cycles of 5 s 95˚C, 5 s 67˚C and 20 s 72˚C (measurement of fluorescence). Melting curve analysis (0 s 95˚C, 12 s 65˚C and 0 s 95˚C) was performed directly after PCR run. Quantification of disseminated tumour cells in mouse blood was based on a standard curve using blood spiked with SK-N-SH neuroblastoma cells grown in culture (1 cell/ml up to 1×10^6 cells/ml).

Statistical analysis. Results of the *in vitro* XTT and modified Scratch assays were compared with an analysis of variance (one-way ANOVA) and Dunnett's post test.
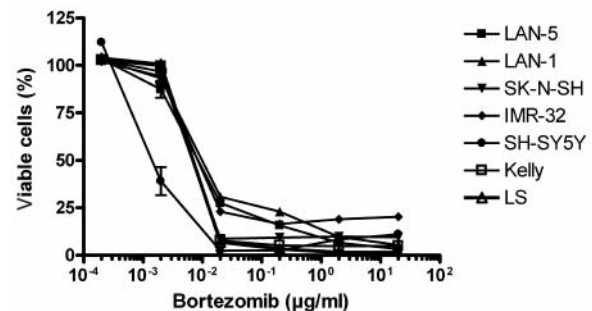

Figure 1. *Effect of bortezomib on the proliferation of seven human neuroblastoma cell lines. Neuroblastoma cell lines were cultured in the presence of various concentrations of bortezomib for 48 h. Cell proliferation was measured by the XTT-based assay kit. Values represent mean±SEM.*

Primary tumour weight, percentage of apoptitic and mitotic cells, and necrotic areas in the primary tumours and number of disseminated tumour cells in the blood of the control and bortezomib treated mice were analysed with the two-tailed Student's *t*-test.

Development of pulmonary metastases in the mice was compared using Fisher's exact test.

All statistical tests were carried out using GraphPad Prism™ software (GraphPad™, San Diego, USA). $P<0.05$ was considered as a statistically significant result.

Results

Cell proliferation. The dose-dependent effect of bortezomib on the cell proliferation of seven human neuroblastoma cell lines is summarized in Figure 1 and Table I. The concentrations from 0.02 to 20 μg/ml bortezomib significantly inhibited cell proliferation of all tested cell lines. Viable cells ranged from 1% to 30% of the control dependent on the respective concentration and cell line. A concentration of 0.002 μg/ml bortezomib inhibited proliferation of SH-SY5Y cells (39% viable cells, $p<0.001$). The other neuroblastoma cells were not significantly influenced by 0.002 μg/ml bortezomib, and 0.0002 μg/ml bortezomib had no relevant effect on cell proliferation of any tested neuroblastoma cell line. IC_{50} of bortezomib of the different neuroblastoma cell lines ranged from 1.2 ng/ml (3.1 nM, SH-SY5Y) to 8.2 ng/ml (21.4 nM, LAN-1) (Table I).
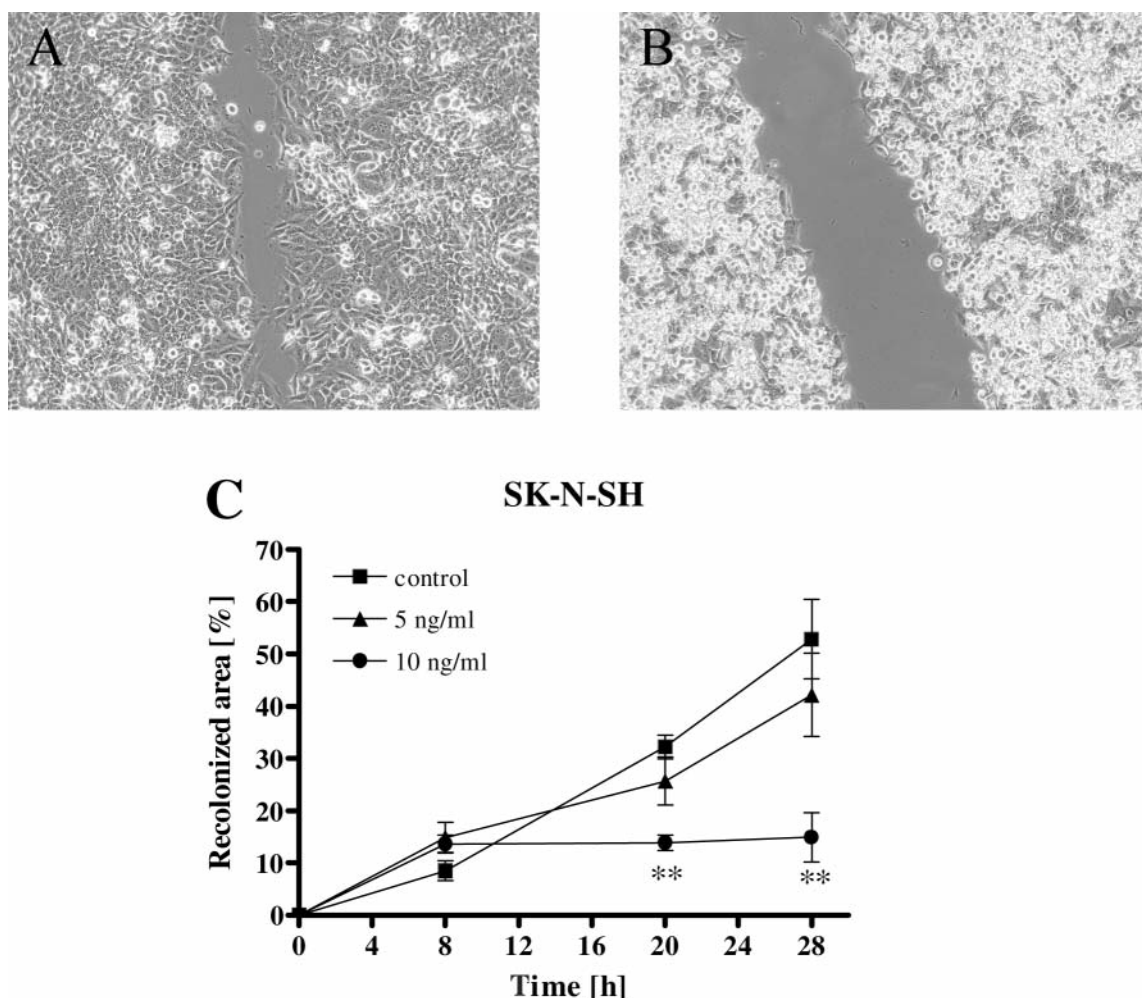
Figure 2. *Bortezomib-mediated effects on scratch wound colonization of SK-N-SH cells. A and B illustrate the cell-free gap 28 h after recolonization by SK-N-SH cells treated with PBS (control, A) and with 10 ng/ml bortezomib (B). C shows the recolonization curves of SK-N-SH cells. Data are presented as means±SEM; **p<0.01; compared to control.*

Cell migration. The migration ability of the bortezomib-treated cells was significantly reduced within a period of 20 to 28 h after treatment ($p<0.01$). The movement of SK-N-SH cells beyond the cell-free gap was not significantly reduced by treatment with 5 ng/ml bortezomib after 20 h (32% control *versus* 26% treated, $p>0.05$) and 28 h (53% control *versus* treated 42%, $p>0.05$). However, treatment with 10 ng/ml bortezomib showed a significant reduction of the migration rate after 20 h (32% control *versus* 14% treated, $p<0.01$) and 28 h (53% control *versus* treated 15%, $p<0.01$) (Figure 2A-C).

Effect of bortezomib in vivo. During the therapeutic study with bortezomib, one SCID mouse of the bortezomib-treated group died from unknown reasons without any obvious reference to the tumour or the tumour therapy. The effects of bortezomib on several parameters of the *in vivo* developed SK-N-SH tumours are summarized in Table II. In the control group, 18 out of 20 (90%) and in the treated group 16 out of 19 (84%) SCID mice developed primary tumours. The mice without primary tumour growth were not considered in the statistical analysis.

Total tumour weight in the control and in the bortezomib group ranged from 0.1 to 0.7 g (mean control 0.32 g, n=18; mean bortezomib 0.33 g, n=16). Five out of the 18 (28%) control mice with primary tumours produced pulmonary metastases, with numbers ranging from 24 to 192 (Figure 3); in contrast no mice in the treatment group (n=16) developed lung metastases ($p<0.05$).

The percentage of apoptotic cells was significantly higher in the treated than in the control tumours (5% control *versus*

Table II. *Effect of bortezomib on growth of human SK-N-SH neuroblastoma cells in a SCID mouse model. Comparison of various parameters between the control and the bortezomib group.*

	Control (n=18)	Bortezomib (n=16)
Tumour weight (g) n.s.	0.32 (±0.05)	0.33 (±0.06)
Pulmonary metastases*	5 of 18 (28%) mice, number of lung metastases: 42; 168; 192; 24; 48.	0 of 16 mice
Percentage of apoptotic cells (%)***	5.0 (±0.18)	10.0 (±0.25)
Percentage of mitotic cells (%)***	6.6 (±0.17)	5.1 (±0.12)
Percentage of necrotic areas (%) n.s.	55.1 (±4.7)	50.5 (±5.5)
Vascular count*	38.4 (±1.3)	32.0 (±1.9)
Disseminated tumour cells in blood (cells/ml) n.s.	1.4 (±0.1)	1.3 (±0.2)

*Values represent mean (±SEM) except for pulmonary metastases. Statistical analysis was performed using Student's t-test and Fisher's exact test for the analysis of pulmonary metastases, respectively. n.s. not significant; *$p < 0.05$; **$p < 0.01$; ***$p < 0.001$.*

10% bortezomib, $p < 0.001$); the rate of mitotic cells was significantly lower in the treated group (6.6% control *versus* 5.1% bortezomib, $p < 0.001$). Furthermore, the mean number of tumour vessels in vital tumour mass treated with bortezomib significantly decreased compared to the control group (38.4 control *versus* 32.0 bortezomib, $p < 0.05$). The necrotic areas (55.1% control *versus* 50.5% bortezomib) and the number of disseminated tumour cells in the blood (1.4 cells/ml control *versus* 1.3 cells/ml bortezomib) did not show any statistically significant difference between the control and the treated group.

Discussion

In the present study, all tested neuroblastoma cell lines showed a dose-dependent inhibition of cell proliferation after treatment with bortezomib. A dose- and time-dependent anti-proliferative effect of bortezomib on several neuroblastoma cells *in vitro* was also demonstrated in some recent studies using different cell lines (22-24, 30). Activation of apoptotic pathways was shown to underlie the cytotoxic effect of bortezomib *in vitro* (30). The effective *in vitro* concentrations of bortezomib in all these studies, including the present study lay in the same order of magnitude.

Cell migration is an important process in tumour cell invasion and local invasion is one of the central steps in the formation of distant metastases. Bortezomib was shown to virtually stop migration of squamous cell cancer at a concentration of 1 μg/ml (31). Furthermore, the low dose combination of bortezomib (3 nM) and a novel proteasome inhibitor NPI-0052 (1 nM) blocked migration of multiple myeloma cells (32). In the present study migration of SK-N-SH cells was significantly inhibited at a concentration of 10 ng/ml bortezomib (25.8 nM) using a modified scratch assay. SK-N-SH cells were chosen because these cells are used in the bortezomib study *in vivo*, because these cells
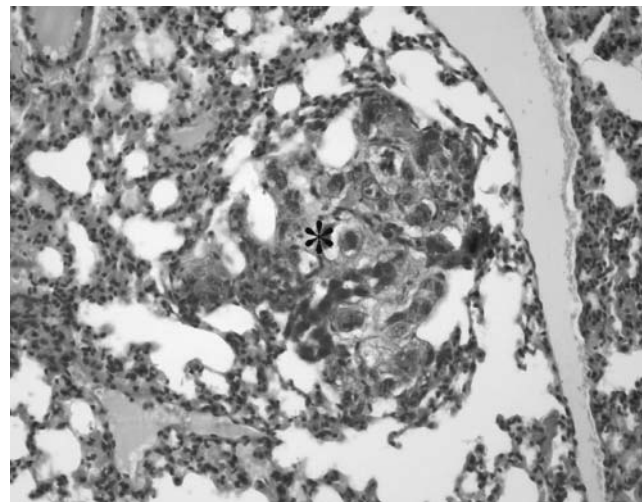

Figure 3. *Pulmonary metastasis (*) of human SK-N-SH neuroblastoma cells engrafted in SCID mice (HE staining).*

have shown a high tumour take-rate and a high metastatic potential in the SCID mouse model after an acceptable time period of growth (33).

Bortezomib was intravenously applied in a concentration of 1 mg/kg twice a week in the *in vivo* study. The median inhibitory concentration in SK-N-SH cells *in vitro* was 5.4 ng/mL bortezomib (14.1 nM), a level that is clinically achievable (34). This dose-rate was adapted to the well-established bortezomib concentrations used in most preclinical and clinical trials (34-36). In the presented experiments, bortezomib had no inhibitory effect on the tumour weight of SK-N-SH cells grown in SCID mice (control 0.32 g *versus* bortezomib 0.33 g). Michaelis *et al*. (24) and Hamner *et al*. (23) demonstrated that bortezomib significantly reduces the tumour volume of the subcutaneously injected neuroblastoma cell lines UKF-NB-

3[r]VCR[10], UKF-NB-3, UKF NB-3[r]Dox[20] and NB-1691. Brignole *et al.* (22) showed that bortezomib restricts the tumour volume of orthotopic injected neuroblastoma SH-SY5Y cells. The use of another neuroblastoma cell line and the different experimental setup may explain the varying effect on neuroblastoma growth *in vivo*. Treatment of mice started three days after the neuroblastoma cell injection in this study, but in the previous reports, tumour cells had grown several days and developed palpable vascularized tumours before application of bortezomib (22-24).

Although the weight of the primary tumours did not significantly differ between the bortezomib and the control group, a statistically significant difference between the two groups was detected with regard to the apoptotic and mitotic rate. Thus, bortezomib induced a duplication of apoptotic cells (5% control *versus* 10% bortezomib, $p<0.001$) and a significant reduction (6.5% control *versus* 5.1% bortezomib, $p<0.001$) of mitotic cells. Michaelis *et al.* (24) also showed that bortezomib reduced the number of mitoses of all tested cell lines *in vivo* and increased the number of apoptotic cells in UKF-NB-3 rVCR10 xenografts. Brignole *et al.* (22) measured apoptosis in the neuroblastomas by TUNEL and stated bortezomib induced apoptosis in tumour tissues. Previous studies assumed that the inhibition of tumour angiogenesis plays an important role for bortezomib-induced neuroblastoma growth inhibition *in vivo* (22-24). In the present study, treatment with bortezomib also produced a significant reduction of MVD.

In this study a specific anti-metastatic effect of bortezomib was demonstrated for the first time since no lung metastases were found in the animals of the treated group, while five mice in the control group developed spontaneous lung metastases ($p<0.05$). This anti-metastatic effect of bortezomib in the neuroblastoma xenograft model corresponds well with the inhibitory effect of bortezomib on cell migration in the scratch assay as cell migration plays a crucial role in the formation of metastases. Hamner *et al.* (23) demonstrated a significant reduction in tumour progression in bortezomib-treated mice with disseminated disease by bioluminescence imaging ($p<0.01$). Furthermore, bortezomib-treated mice with disseminated neuroblastomas lived significantly longer than control mice (control 50.3 days *versus* bortezomib 74.2 days, $p<0.001$) (22). In a syngeneic model of transplantable murine neuroblastoma, bortezomib potentiated the growth inhibitory effects of cytokine treatment in mice with metastatic disease (36). However, in these reports the anti-metastatic effect of bortezomib was tested by injecting the tumour cells into the tail vein, which represents dissemination rather than metastasis. In the present study, SK-N-SH cells were subcutaneously injected between the scapulae of SCID mice, so that the tumour cells had to pass each stage of the multistep phenomenon of metastasis in order to develop pulmonary metastases. The number of disseminated human neuroblastoma cells in the blood of SCID mice was determined in the present study by real-time PCR, showing no difference between the treated and the control group. However, only one blood sample was taken at the end of the experiment restricting the significance of this result.

In conclusion, bortezomib has a significant inhibitory effect on cell proliferation of human neuroblastoma cells *in vitro* as well as pro-apoptotic, anti-mitotic, anti-angiongenic and anti-metastatic effects in a SCID mouse model. These results and the disappointing survival rates of children with metastatic neuroblastoma provide a rationale to make further investigations of bortezomib in the treatment of neuroblastoma.

References

1 Morgenstern BZ, Krivoshik AP, Rodriguez V and Anderson PM: Wilms' tumor and neuroblastoma. Acta Paediatr Suppl *93*: 78-85, 2004.

2 Berthold F, Hero B, Kremens B, Handgretinger R, Henze G, Schilling FH, Schrappe M, Simon T and Spix C: Long-term results and risk profiles of patients in five consecutive trials (1979-1997) with stage 4 neuroblastoma over 1 year of age. Cancer Lett *197*: 11-17, 2003.

3 De Bernardi B, Nicolas B, Boni L, Indolfi P, Carli M, Cordero Di Montezemolo L, Donfrancesco A, Pession A, Provenzi M, di Cataldo A, Rizzo A, Tonini GP, Dallorso S, Conte M, Gambini C, Garaventa A, Bonetti F, Zanazzo A, D'Angelo P and Bruzzi P: Disseminated neuroblastoma in children older than one year at diagnosis: comparable results with three consecutive high-dose protocols adopted by the Italian Co-Operative Group for Neuroblastoma. J Clin Oncol *21*: 1592-1601, 2003.

4 Maris JM, Hogarty MD, Bagatell R and Cohn SL: Neuroblastoma. Lancet *369*: 2106-2120, 2007.

5 Schumacher U and Adam E: Lectin histochemical HPA-binding pattern of human breast and colon cancers is associated with metastases formation in severe combined immunodeficient mice. Histochem J *29*: 677-684, 1997.

6 Schumacher U and Mitchell BS: Use of clinically relevant human-scid-mouse models in metastasis research. Trends Biotechnol *15*: 239-241, 1997.

7 Thies A, Mauer S, Fodstad O and Schumacher U: Clinically proven markers of metastasis predict metastatic spread of human melanoma cells engrafted in scid mice. Br J Cancer *96*: 609-616, 2007.

8 Valentiner U, Hall DM, Brooks SA and Schumacher U: HPA binding and metastasis formation of human breast cancer cell lines transplanted into severe combined immunodeficient (scid) mice. Cancer Lett *219*: 233-242, 2005.

9 Adams J: The development of proteasome inhibitors as anticancer drugs. Cancer Cell *5*: 417-421, 2004.

10 Richardson PG and Anderson KC: Bortezomib: a novel therapy approved for multiple myeloma. Clin Adv Hematol Oncol *1*: 596-600, 2003.

11 Adams J: The proteasome: structure, function, and role in the cell. Cancer Treat Rev *29(Suppl 1)*: 3-9, 2003.

12 Adams J, Palombella VJ, Sausville EA, Johnson J, Destree A, Lazarus DD, Maas J, Pien CS, Prakash S and Elliott PJ: Proteasome inhibitors: a novel class of potent and effective antitumor agents. Cancer Res *59*: 2615-2622, 1999.

13 Bold RJ, Virudachalam S and McConkey DJ: Chemosensitization of pancreatic cancer by inhibition of the 26S proteasome. J Surg Res *100*: 11-17, 2001.

14 Frankel A, Man S, Elliott P, Adams J and Kerbel RS: Lack of multicellular drug resistance observed in human ovarian and prostate carcinoma treated with the proteasome inhibitor PS-341. Clin Cancer Res *6*: 3719-3728, 2000.

15 Hideshima T, Richardson P, Chauhan D, Palombella VJ, Elliott PJ, Adams J and Anderson KC: The proteasome inhibitor PS-341 inhibits growth, induces apoptosis, and overcomes drug resistance in human multiple myeloma cells. Cancer Res *61*: 3071-3076, 2001.

16 Ling YH, Liebes L, Jiang JD, Holland JF, Elliott PJ, Adams J, Muggia FM and Perez-Soler R: Mechanisms of proteasome inhibitor PS-341-induced G(2)-M-phase arrest and apoptosis in human non-small cell lung cancer cell lines. Clin Cancer Res *9*: 1145-1154, 2003.

17 Olivier S, Robe P and Bours V: Can NF-kappaB be a target for novel and efficient anticancer agents? Biochem Pharmacol *72*: 1054-1068, 2006.

18 Pham LV, Tamayo AT, Yoshimura LC, Lo P and Ford RJ: Inhibition of constitutive NF-kappa B activation in mantle cell lymphoma B cells leads to induction of cell cycle arrest and apoptosis. J Immunol *171*: 88-95, 2003.

19 Shah SA, Potter MW, McDade TP, Ricciardi R, Perugini RA, Elliott PJ, Adams J and Callery MP: 26S proteasome inhibition induces apoptosis and limits growth of human pancreatic cancer. J Cell Biochem *82*: 110-122, 2001.

20 Sunwoo JB, Chen Z, Dong G, Yeh N, Crowl Bancroft C, Sausville E, Adams J, Elliott P and Van Waes C: Novel proteasome inhibitor PS-341 inhibits activation of nuclear factor-kappa B, cell survival, tumor growth, and angiogenesis in squamous cell carcinoma. Clin Cancer Res *7*: 1419-1428, 2001.

21 Van Waes C, Chang AA, Lebowitz PF, Druzgal CH, Chen Z, Elsayed YA, Sunwoo JB, Rudy SF, Morris JC, Mitchell JB, Camphausen K, Gius D, Adams J, Sausville EA and Conley BA: Inhibition of nuclear factor-kappaB and target genes during combined therapy with proteasome inhibitor bortezomib and reirradiation in patients with recurrent head-and-neck squamous cell carcinoma. Int J Radiat Oncol Biol Phys *63*: 1400-1412, 2005.

22 Brignole C, Marimpietri D, Pastorino F, Nico B, Di Paolo D, Cioni M, Piccardi F, Cilli M, Pezzolo A, Corrias MV, Pistoia V, Ribatti D, Pagnan G and Ponzoni M: Effect of bortezomib on human neuroblastoma cell growth, apoptosis, and angiogenesis. J Natl Cancer Inst *98*: 1142-1157, 2006.

23 Hamner JB, Dickson PV, Sims TL, Zhou J, Spence Y, Ng CY and Davidoff AM: Bortezomib inhibits angiogenesis and reduces tumor burden in a murine model of neuroblastoma. Surgery *142*: 185-191, 2007.

24 Michaelis M, Fichtner I, Behrens D, Haider W, Rothweiler F, Mack A, Cinatl J, Doerr HW and Cinatl J Jr: Anticancer effects of bortezomib against chemoresistant neuroblastoma cell lines *in vitro* and *in vivo*. Int J Oncol *28*: 439-446, 2006.

25 Kerr JF, Wyllie AH and Currie AR: Apoptosis: a basic biological phenomenon with wide-ranging implications in tissue kinetics. Br J Cancer *26*: 239-257, 1972.

26 Hall PA: Assessing apoptosis: a critical survey. Endocr Relat Cancer *6*: 3-8, 1999.

27 Sharma R, Adam E and Schumacher U: The action of 5-fluorouracil on human HT29 colon cancer cells grown in SCID mice: mitosis, apoptosis and cell differentiation. Br J Cancer *76*: 1011-1016, 1997.

28 Jojovic M and Schumacher U: Quantitative assessment of spontaneous lung metastases of human HT29 colon cancer cells transplanted into SCID mice. Cancer Lett *152*: 151-156, 2000.

29 Schneider T, Osl F, Friess T, Stockinger H and Scheuer WV: Quantification of human Alu sequences by real-time PCR – an improved method to measure therapeutic efficacy of anti-metastatic drugs in human xenotransplants. Clin Exp Metastasis *19*: 571-582, 2002.

30 Combaret V, Boyault S, Iacono I, Brejon S, Rousseau R and Puisieux A: Effect of bortezomib on human neuroblastoma: analysis of molecular mechanisms involved in cytotoxicity. Mol Cancer *7*: 50, 2008.

31 Lorch JH, Thomas TO and Schmoll HJ: Bortezomib inhibits cell-cell adhesion and cell migration and enhances epidermal growth factor receptor inhibitor-induced cell death in squamous cell cancer. Cancer Res *67*: 727-734, 2007.

32 Chauhan D, Singh A, Brahmandam M, Podar K, Hideshima T, Richardson P, Munshi N, Palladino MA and Anderson KC: Combination of proteasome inhibitors bortezomib and NPI-0052 trigger *in vivo* synergistic cytotoxicity in multiple myeloma. Blood *111*: 1654-1664, 2008.

33 Valentiner U, Valentiner FU and Schumacher U: Expression of CD44 is associated with a metastatic pattern of human neuroblastoma cells in a SCID mouse xenograft model. Tumour Biol *29*: 152-160, 2008.

34 Rajkumar SV, Richardson PG, Hideshima T and Anderson KC: Proteasome inhibition as a novel therapeutic target in human cancer. J Clin Oncol *23*: 630-639, 2005.

35 Boccadoro M, Morgan G and Cavenagh J: Preclinical evaluation of the proteasome inhibitor bortezomib in cancer therapy. Cancer Cell Int *5*: 18, 2005.

36 Khan T, Stauffer JK, Williams R, Hixon JA, Salcedo R, Lincoln E, Back TC, Powell D, Lockett S, Arnold AC, Sayers TJ and Wigginton JM: Proteasome inhibition to maximize the apoptotic potential of cytokine therapy for murine neuroblastoma tumors. J Immunol *176*: 6302-6312, 2006.